Published in final edited form as:
Cancer Biol Ther. 2009 August ; 8(16): 1587–1595.

Mcl1 downregulation sensitizes neuroblastoma to cytotoxic chemotherapy and small molecule Bcl2-family antagonists

Brian J. Lestini[1,2], **Kelly C. Goldsmith**[1,2], **Mark N. Fluchel**[3], **Xueyuan Liu**[1], **Niel L. Chen**[1], **Bella Goyal**[1], **Bruce R. Pawel**[4], and **Michael D. Hogarty**[1,2,*]

[1]Division of Oncology; The Children's Hospital of Philadelphia; Philadelphia, PA USA

[2]Department of Pediatrics, University of Pennsylvania School of Medicine; Philadelphia, PA USA

[3]Department of Pediatrics; Primary Children's Hospital; University of Utah; Salt Lake City, UT USA

[4]Department of Pathology and Laboratory Medicine; University of Pennsylvania School of Medicine; Philadelphia, PA USA

Abstract

Neuroblastoma (NB) is a common, highly lethal pediatric cancer, with treatment failures largely attributable to the emergence of chemoresistance. The pro-survival Bcl2 homology (BH) proteins critically regulate apoptosis, and may represent important therapeutic targets for restoring drug sensitivity in NB. We used a human NB tumor tissue microarray to survey the expression of pro-survival BH proteins Mcl1 and Bcl2, and correlated expression to clinical prognostic factors and survival. Primary NB tumors heterogeneously expressed Mcl1 or Bcl2, with high expression correlating to high-risk phenotype. Co-expression is infrequent (11%), but correlates to reduced survival. Using RNA interference, we investigated the functional relevance of Mcl1 and Bcl2 in high-risk NB cell lines (SK-N-AS, IMR-5, NLF). Mcl1 knockdown induced apoptosis in all NB cell lines, while Bcl2 knockdown inhibited only NLF, suggesting functional heterogeneity Finally, we determined the relevance of Mcl1 in resistance to conventional chemotherapy (etoposide, doxorubicin) and small molecule Bcl2-family antagonists (ABT-737 and AT-101). Mcl1 silencing augmented sensitivity to chemotherapeutics 2- to 300-fold, while Bcl2 silencing did not, even in Bcl2-sensitive NLF cells. Resistance to ABT-737, which targets Bcl2/-w/-x, was overcome by Mcl1 knockdown. AT-101, which also neutralizes Mcl1, had single-agent cytotoxicity, further augmented by Mcl1 knockdown. In conclusion, Mcl1 appears a predominant pro-survival protein contributing to chemoresistance in NB, and Mcl1 inactivation may represent a novel therapeutic strategy. Optimization of compounds with higher Mcl1 affinity, or combination with additional Mcl1 antagonists, may enhance the clinical utility of this approach.

Keywords

embryonal tumors; Bcl2 family; oncogene; experimental therapeutics; Bcl2 antagonists; neuroblastoma; Mcl1

*Correspondence to: Michael D. Hogarty; Division of Oncology; The Children's Hospital of Philadelphia; 9 North ARC; Suite 902C; 3615 Civic Center Boulevard; Philadelphia, PA 19104-4318 USA; Tel.: 215.590.3931; Fax: 215.590.3770; hogartym@email.chop.edu.

Supplementary materials can be found at: www.landesbioscience.com/supplement/LestiniCBT8-16-Sup.pdf

Introduction

Despite maximally intensive multimodal therapy, high-risk neuroblastoma (NB) remains a significant cause of pediatric cancer mortality. Relapse after initial response to therapy is the major reason for treatment failure. Implied is the acquisition and selection of therapy-resistant cells that evade apoptotic stimuli. Prior studies demonstrate that NB-derived cells maintain competent mitochondrial apoptotic signaling,[1–3] and are dependent on these pathways for response to diverse cellular stressors such as MycN overexpression or cytotoxic agents.[4–6] Entry into the final common pathway of mitochondrial apoptosis is governed by competitive binding of pro-death Bcl2 homology (BH) proteins to multi-domain pro-survival BH members such as Mcl1 and Bcl2, effectively neutralizing activation of pro-death Bak and/or Bax. Chemoresistance may derive from the activation of pro-survival BH proteins, which tip the cellular balance away from apoptosis as demonstrated for Bcl2 in numerous cancer models.[7,8]

Mcl1 is a pro-survival BH protein implicated in the pathogenesis and resistance of diverse malignancies. Mcl1 antagonism has shown preclinical anti-tumor activity in myeloma, lymphoma, melanoma, sarcoma, and small and non-small cell lung cancer,[9–13] and multiple Phase I and II clinical trials of small molecule Mcl1 antagonists currently are underway. Several lines of indirect evidence suggest *MCL1* also may function as a putative oncogene in NB. First, *MCL1* maps within 1q21, a region of genomic copy number gain encountered in a large proportion of human NB cell lines and primary NB tumors and associated with worse outcome.[14,15] Gain within murine chromosome 3 (encompassing the murine Mcl1 orthologue) also is seen in NB arising in the transgenic *TH-MYCN* mouse model (ref. 16 and W. Weiss, personal communication). Secondly, Mcl1 appears to lie downstream of TRAIL induced apoptosis mediated by NFκB. Finally, using a *MYCN*-inducible neural cell model, we have selected for apoptosis-resistant cells that upregulate Mcl1 (Hogarty M, manuscript in preparation). Together these findings suggest that Mcl1 may contribute to oncogenesis in NB by impeding apoptosis, and may act to inhibit apoptotic stimuli downstream of dysregulated MycN.

In this study, we sought to delineate the relative roles of Mcl1 and Bcl2 in NB survival, and to determine if BH silencing altered sensitivity to conventional cytotoxic agents and to targeted Bcl2-family antagonists. A human tumor tissue microarray (TMA) was utilized to broadly assess expression, and to correlate expression to clinical features. Subsequently, we used RNA interference (RNAi) to selectively knockdown individual pro-survival BH proteins in diverse NB-derived cell lines with variable “addiction” to distinct BH proteins (Goldsmith K, submitted). Mcl1 antagonism induced growth inhibition in all cell lines. Further, sensitivity to cytotoxic chemotherapy and to small molecule BH antagonists (ABT-737 and/or AT-101) in resistant cells was augmented by Mcl1 silencing, suggesting that Mcl1 provides an important functional barrier to apoptosis. These results have therapeutic implications for translating emerging Bcl2-family antagonists into clinical use for the treatment of chemoresistant NB.

Results

Mcl1 and Bcl2 are differentially expressed in primary NB

Of 185 primary human neuroblastomas comprising the TMA, 134 were evaluable for Mcl1 staining, and 154 for Bcl2. Tumors were heterogeneous in expression of each protein (Fig. 1). Semi-quantitative scoring demonstrated that Mcl1 or Bcl2 expression was present in a majority (57%) of tumors (Table 1). Thirty-one percent stained exclusively for Mcl1, and 31% for Bcl2. Notably, there was infrequent overlap, with 11% of NBs expressing detectable levels of both proteins. Twenty-seven percent demonstrated high levels of

expression (as defined in Methods): high levels of Mcl1 alone were seen in 13%, and Bcl2 alone in 16%. Again, a small percentage (5%) highly expressed both proteins, indicating differential expression of anti-apoptotic proteins across tumors.

One hundred-one tumors were from patients of known Children's Oncology Group (COG) risk group status. Thirty-five percent were high-risk, 22% were intermediate-risk, and 44% were low-risk. Eighty-one percent of high-risk tumors expressed either Mcl1 or Bcl2 (Table 1). This represented a significantly higher proportion than seen in intermediate- or low (IL)-risk tumors ($p = 0.05$). Expression of Mcl1 was consistent across risk groups at ~40%, whereas Bcl2 expression was significantly higher in high-risk tumors (50%) compared with those of IL-risk (25%; $p = 0.02$). A smaller number of IL-risk tumors (11%) stained for both Mcl1 and Bcl2, compared with ~20% of high-risk NBs, although statistical significance was not achieved with this sample size.

NBs with *MYCN* amplification expressed significantly higher levels of Mcl1 than nonamplified NBs (40% vs. 11%; $p = 0.03$). This difference was not seen for Bcl2 (21% for *MYCN* amplified vs. 18%; $p = 0.72$). *MYCN* amplified tumors also tended to have high levels of at least one BH protein when compared with nonamplified NBs (55% vs. 25%; $p = 0.07$). Ten percent of *MYCN* amplified tumors highly expressed both Mcl1 and Bcl2, compared with 5% for nonamplified tumors ($p = 0.48$). Together, TMA data demonstrate that pro-survival BH proteins are expressed in a large portion of human NB tumors, and their abundance correlates to high-risk features. Expression patterns appear heterogeneous and are typically exclusive, with relatively few tumors demonstrating high expression of both Mcl1 and Bcl2.

Survival analysis demonstrated expected outcomes for known prognostic factors of COG risk group and *MYCN* amplification status as described in larger, unselected series (Suppl. Fig. 1), suggesting a representative sampling on the TMA. Subsequently, we analyzed survival on the basis of Mcl1 and/or Bcl2 expression. A statistically significant difference in overall survival (OS) was seen in patients whose tumors expressed both Mcl1 and Bcl2 ($p = 0.04$; Fig. 1D), with similar median length of follow-up for the two groups (4.7 years vs. 4.9 years). Also, patients whose tumors expressed at least one pro-survival protein trended toward worse OS (Suppl. Fig. 1). Whether expression levels were scored as high or low did not carry significance for either protein.

Gene silencing of Mcl1 and Bcl2 differentially impacts NB viability

We selected three representative NB-derived cell lines for RNAi functional studies. SK-N-AS was derived post-therapy, lacks *MYCN* amplification, and is p53 defective.[18] Both IMR-5 and NLF were obtained prior to therapy, and are *MYCN* amplified. Assessment of basal BH protein expression across cell lines showed abundant constitutive Mcl1 expression, including neural RPE1 control cells, while Bcl2 expression was present but variable (Suppl. Fig. 2A). These findings are consistent with observations in an expanded panel of high-risk primary NBs (Goldsmith K, submitted).

Cells were transiently transfected with small inhibitory RNAs (siRNA) in vitro, and viable cell number was assessed over time. Quantitative real-time reverse transcriptase polymerase chain reaction (Q-RT-PCR) confirmed transfection, with selective mRNA knockdown of 50–93% (Suppl. Fig. 2B). The lowest transfection efficiency was seen in IMR-5; however, mRNA levels were still reduced at least 50% for each target. Mcl1 knockdown resulted in effective cell killing of each NB cell line in the absence of concomitant apoptotic stimuli, at siRNA concentrations as low as 5 nM (Fig. 2A). A modest but consistent dose response was observed toward 100 nM (Suppl. Fig. 3). To minimize potential off-target effects, we utilized 5 nM siMCL1 for subsequent experiments. The kinetics of siMCL1 induced cell

death appeared to differ across cell lines. A decline in CI was observed within 12–24 hours of siRNA addition for SK-N-AS and IMR-5, indicating rapid turnover of protein and a strong dependence on Mcl1 for survival. NLF showed a more gradual response in the initial 48 hours post-transfection, although near-complete loss of cell viability was observed by 72 hours. No effect of Mcl1 knockdown was seen in control RPE1 cells despite efficient transfection, suggesting that NB cell lines are preferentially dependent on Mcl1 for viability.

Bcl2 reduction had no effect on the growth or survival of SK-N-AS or IMR-5 cells at siRNA concentrations up to 100 nM (Fig. 2A and Suppl. Fig. 3). A compensatory increase in Mcl1 mRNA was not seen, suggesting that increased Mcl1 transcription does not account for lack of response to Bcl2 knockdown (Suppl. Fig. 4). In contrast, NLF did show partial dependence on Bcl2 for survival, as knockdown inhibited viable cell number over time. Again, no effect on growth of RPE1 was observed with Bcl2 reduction.

Whole cell immunoblots confirmed decreased protein levels for both Mcl1 and Bcl2 in knockdown specimens, as measured 48 hours after transfection (Fig. 2B). These results are particularly important for an appropriate functional interpretation, as the half-life of Mcl1 is much shorter than that of Bcl2. Target protein reduction was nearly complete in SK-N-AS and NLF, yet a functional disparity existed between Mcl1 and Bcl2. For example, SK-N-AS survival was markedly diminished with Mcl1 reduction, while a similar degree of Bcl2 reduction had no impact on cell growth. IMR-5 retained more target protein at 48 hours. This likely reflects the slightly lower siRNA transfection efficiency in this cell line, although alterations in protein stability cannot be excluded. Nonetheless, IMR-5 still showed dramatic growth inhibition with Mcl1 knockdown, but not with Bcl2. From these data, we conclude that Mcl1 appears to play a predominant role (as compared to Bcl2) in suppressing cell death in SK-N-AS and IMR-5. In contrast, Mcl1 appears redundant with Bcl2 in NLF. These findings support a functional heterogeneity in NB for pro-survival BH protein dependence.

To investigate the mechanism of cellular response to pro-survival BH knockdowns, we conducted parallel siRNA experiments to examine cell morphology by phase microscopy and mitochondrial apoptosis by caspase-9 cleavage. siMcl1-treated SK-N-AS cells assumed a highly refractile, rounded and fragmented morphology consistent with apoptosis (Fig. 2C, upper) that temporally correlated to reductions in viable cell number detected by Real-Time Cellular Electronic Sensing (RT-CES) cell proliferation assay. In contrast, knockdown of Bcl2 or GapDH had no effect on morphology (Fig. 2C, lower). Analogous findings were observed for IMR-5 and NLF, with the exception that Bcl2 knockdown in NLF induced apoptotic morphology consistent with the Bcl2 dependence seen by RT-CES (not shown). Protein immunoblotting demonstrated complete degradation of full-length 47 kDa caspase-9 in siMcl1 transfected SK-N-AS, along with generation of a 37 kDa cleavage product indicative of apoptosome activation (Fig. 2D). Of note, SK-N-AS cells transfected with siGDH also demonstrated some cleavage product, but retained substantial full-length caspase-9 as well. No caspase-9 processing was seen following Bcl2 reduction in this cell line, consistent with cell proliferation data. These findings were similar for IMR-5 cells; although the degree of caspase-9 degradation was less striking for Mcl1 knockdown than in SK-N-AS, processing was apparent in multiple replicates. NLF cells demonstrated nearly complete caspase-9 cleavage following Mcl1 reduction, and substantial caspase-9 cleavage following Bcl2 reduction, consistent with findings from cell viability assays. NLF cells also demonstrate the 37 kDa cleavage product even in untreated cells, indicating some basal caspase-9 processing at steady state. Nonetheless, additional caspase-9 processing in concert with morphologic hallmarks of apoptosis was seen only in siMcl1 or siBcl2 treated cells. These data support the notion that reduced NB viability following BH knockdown proceeds through apoptosome signaling.

Mcl1 silencing sensitizes NB cell lines to conventional cytotoxic agents

If the mitochondrial apoptotic machinery in NB is intact but suppressed by pro-survival BH proteins, we reasoned that downregulating these proteins might restore chemosensitivity in resistant cells. SK-N-AS and NLF cells were selected for study as they represented cell lines that demonstrated efficient protein silencing and differential dependence on Mcl1 and Bcl2. Furthermore, SK-N-AS cells are chemoresistant, presumably attributable to defective p53 function.[18] siRNA targeting of Mcl1 or Bcl2 was followed 24 hours later by chemotherapy, at exposures selected near or below 48-hour $IC5_0$ values determined by MTT assay in the absence of siRNA (Fig. 3 and data not shown). We used 5 nM siMCL1 to minimize off-target effects and to provide a broader dynamic range for chemotherapy responses. Additionally, at the time of chemotherapy addition siRNA was not replenished, to diminish any possible confounding effect of tonic repression.

SK-N-AS underwent apoptosis at concentrations of etoposide >2-log below the monotherapy IC_{50} (Fig. 3A, left). This effect was not seen in cells treated with a combination of drug and siGDH, nor with siMCL1 alone. A similar effect was seen with doxorubicin (Fig. 3A, right). Concentrations 6-fold lower than the monotherapy IC_{50} were cytotoxic in the setting of Mcl1 knockdown. Statistically significant differences in cell survival were apparent when combining chemotherapy with Mcl1 knockdown (Fig. 3B, upper). Note that data are normalized to siMCL1 or siGDH treatment alone; therefore, the additional cell killing seen with combination treatment reflects an interaction (i.e., additivity or synergism) between Mcl1 knockdown and chemotherapy. Further consistent with functional RNAi data in SK-N-AS, no augmentation of cytotoxicity was observed with knockdown of Bcl2, despite a higher Bcl2 siRNA concentration (50 nM). If anything, Bcl2 knockdown provided a modest but consistent cytoprotective effect (Fig. 3B, lower).

We next performed these studies with NLF cells, which had demonstrated dependence on both Mcl1 and Bcl2 by RNAi. As in SK-N-AS, etoposide-induced death of NLF was enhanced by Mcl1 knockdown at an etoposide concentration 25-fold lower than the IC_{50} (Fig. 3C). Enhanced doxorubicin cytotoxicity was also observed. Although siBCL2 alone induced growth inhibition, we observed only modest enhancement of cytotoxicity with Bcl2 knockdown that generally did not reach statistical significance (Fig. 3D). These data support the notion that, although both Bcl2 and Mcl1 promote survival in NLF cells, Mcl1 predominantly contributes to chemoresistance.

Sensitivity of NB cell lines to small molecule BH antagonism, and Mcl1 mediated resistance to ABT-737

We next assessed an alternate, clinically feasible mode of pro-survival BH antagonism, using small molecule agents that competitively bind and neutralize Bcl2-family proteins. These therapeutics have differing affinities for BH family members and antagonize restricted subsets.[19] ABT-737 is a Bad-like molecule that binds with subnanomolar affinity to Bcl2, Bcl-w and Bcl-xL, but has no appreciable affinity for Mcl1 or A1/Bfl.[20] Its orally bioavailable analog, ABT-263, recently was tested against NB in vitro and in vivo, but demonstrated limited activity.[21] As resistance to ABT-737 may be mediated by Mcl1,[22–25] we tested the in vitro sensitivity of SK-N-AS and NLF to ABT-737, alone and in combination with Mcl1 knockdown.

SK-N-AS cells were resistant to ABT-737 over a concentration range of 0.2–10 μM (Fig. 4A, left), consistent with previously tested NB cell lines.[21] However, when cells are transfected with siMCL1 prior to ABT-737 exposure, sensitivity is augmented approximately 2 logs (Fig. 4A, middle and right). Cytotoxic effects were rapid, noted 20 minutes post-drug exposure. NLF cells were more sensitive to ABT-737, but still had an

IC_{50} of ~10–20 μM (Fig. 4B, left). Mcl1 knockdown again led to profound sensitization (Fig. 4B, middle and right). To control for possible transfection condition effects on cell permeability, siGDH transfected cells were treated similarly, with no cytotoxic drug activity seen at concentrations <20 μM (not shown).

Prior studies have shown that compensatory upregulation of Mcl1 contributes to ABT-737 resistance in lymphoid malignancies.[23] We therefore investigated Mcl1 levels in untreated SK-N-AS cells, versus cells treated for 6 hours with increasing concentrations of ABT-737. No significant alteration in Mcl1 levels was observed above the substantial basal level of expression (Fig. 4C). While Mcl1 levels may increase further at later time points, our data support that constitutive upregulation of Mcl1 is the predominant mechanism of resistance to ABT-737, and that drug activity is restored if Mcl1 is simultaneously antagonized.

The functional differences in pro-survival BH dependence observed by RNAi, and the marked sensitization to ABT-737 with concomitant Mcl1 knockdown, suggested that Mcl1 dependent NB cells might be more susceptible to small molecule antagonists that target Mcl1. AT-101 is a negative enantiomer of gossypol, with broad affinity for pro-survival BH proteins including Mcl1 (K_i ~180 nM).[26] We therefore tested the activity of AT-101 against SK-N-AS and NLF. As predicted by RNAi, AT-101 demonstrated activity in SK-N-AS and NLF at low-micromolar concentrations (Fig. 5A and B). Pretreatment with siMCL1 further augmented AT-101 cytotoxicity, most evident at early time points (Fig. 5C and D), although this was not as dramatic as with Mcl1 knockdown prior to ABT-737 exposure. The augmented cytotoxicity observed with Mcl1 knockdown supports the hypothesis that small molecule Bcl2-family antagonists with higher Mcl1 affinity might show increased activity in NB.

Discussion

Development of chemoresistance is responsible for the majority of treatment failures in NB. This process is complex, involving loss of cell cycle checkpoint integrity including defects in p53 or p73,[18,27,28] induction of drug efflux pathways via MDR[29] and evasion of programmed cell death through defective apoptotic signaling,[1] among others. The majority of data indicate that properly stimulated NB cells retain the capacity to engage mitochondrial apoptosis, but that the threshold for signal transduction (governed by BH proteins) is heightened.[30] Therefore, we hypothesized that gain of pro-survival BH protein function is one mechanism contributing to a resistant phenotype.

Using a NB tumor TMA, we show that primary NBs express Bcl2 or Mcl1 rather reciprocally, and that expression correlates to high-risk features. Dual expression is restricted to a subset with exceptionally poor overall survival, consistent with the observation that NB-derived cell lines (which establish preferentially from patients with highest risk disease) co-express Bcl2 and Mcl1 frequently. This result bears independent validation, and it will be interesting to determine whether co-expression is more prevalent in matched tumors derived at diagnosis and relapse. Overall, Bcl2 expression correlated to high-risk NB, while Mcl1 was expressed across risk groups. However, high Mcl1 was associated with *MYCN* amplification, consistent with a posited role in abrogating *MYC*-mediated apoptosis.[6,31]

In addition to expression heterogeneity, RNAi studies demonstrate functional pro-survival heterogeneity. Mcl1 knockdown consistently engaged apoptosis in the absence of exogenous stressors, whereas Bcl2 knockdown showed only modest cytotoxicity limited to NLF. Importantly, Mcl1 reduction led to marked chemosensitization in each cell line. Although RNAi has yet to be optimized for clinical use, the technique provides an accurate bioprobe

to assess contributions from individual BH proteins, and these results suggest Mcl1 plays a predominant role in cell survival and chemoresponsiveness. Interestingly, SK-N-AS harbors mutated p53, which under wild-type conditions upregulates the pro-death BH3 proteins Noxa and Puma in response to apoptotic stress.[32] Our data demonstrate that Mcl1 abrogates the response to DNA damaging agents, suggesting that Mcl1 might be a mechanism of apoptosis avoidance in the setting of altered p53 function. Although the majority of NBs do not contain mutations in *TP53* at diagnosis, it has been hypothesized that defective p53 plays a role in relapse or progression. [27,33] While the exact role of Mcl1 in p53 deficient NB models remains to be elucidated experimentally, it is conceivable that a relative abundance of Mcl1 overwhelms the ability of sensitizing BH3 proteins to effectively compete for Bim or Bak binding, thus contributing to chemoresistance. This is supported by the observation that Noxa levels increase with proteasome inhibition and correlate to bortezomib cytotoxicity,[11] and that Noxa upregulation overcomes resistance to ABT-737 in colorectal cancer.[34] Of note, we saw no cytotoxicity against non-transformed neural RPE1 cells with any BH antagonist approach. These findings are consistent with the notion that NB cells may be “primed” for apoptosis through tonically engaged death programs, which are efficiently repressed by pro-survival proteins at steady state.[8]

Since its discovery in follicular lymphoma, Bcl2 and related family members have been shown to play a primary role in the initiation and progression of many hematologic and solid malignancies. Consequently, small molecules that antagonize the operative pro-survival BH proteins have demonstrated pre-clinical activity, alone or in combination with conventional chemotherapeutics.[10,11,35] An Mcl1 antisense (ASO) approach demonstrated sensitization of liposarcoma cells to low dose cyclophosphamide, despite no objective response to ASO or drug alone.[12] In pancreatic carcinoma, Mcl1-directed RNAi augmented response to gemcitabine.[36] Finally, Mcl1 as a resistance mechanism to ABT-737 is now well recognized. [20,23] In total, specific Mcl1-directed therapies appear to restore sensitivity in tumor models that rely on Mcl1 for survival.

Our studies demonstrate that two Bcl2-family antagonists, ABT-737 and AT-101, induce NB cell death in a manner consistent with their known relative affinities, and with cell line-specific BH dependence defined by genetic knockdown. ABT-737 most clearly acts through BH protein antagonism, requiring intact Bak/Bax for cytotoxicity.[24] NLF, which was inhibited by Bcl2 knockdown, was more sensitive to ABT-737 than SK-N-AS, though activity was modest in both cell lines. Importantly, Mcl1 knockdown markedly enhanced ABT-737 activity in both, suggesting that resistance is mediated at least partly by Mcl1. We did not test the contribution of other pro-survival family members (Bcl-x_L, Bcl-w, Bcl-B or A1/Bfl); however, the magnitude of sensitization seen with Mcl1 silencing supports a prominent functional role.

AT-101 has pro-survival antagonism as a major mechanism of action, but at higher concentrations may induce cytotoxicity via alternative pathways.[20,24], In contrast to ABT-737, which selectively antagonizes a subset of BH proteins, AT-101 is more broadly avid and, importantly, neutralizes Mcl1. As predicted by RNAi, single agent AT-101 was more active against the NB cells tested, with an IC_{50} in the low micromolar range. Of note, concomitant Mcl1 knockdown further increased potency, suggesting that Mcl1 antagonism is incomplete, and that further optimization of compounds to antagonize Mcl1 may be warranted.

A recent study by the pediatric preclinical testing program demonstrated that Bcl2/-w/-x antagonists such as ABT-263 or ABT-737 may have limited single-agent activity in NB.[21] Our data now demonstrate that NB cells frequently harbor a functional dependence on Mcl1, and that Mcl1 antagonism induces apoptosis and enhances cytotoxicity. As antagonism with

the Bcl2-family small molecules is potent and highly specific, activity may be enhanced by combination therapies that antagonize Mcl1. Additionally, we show that AT-101 may have clinical utility, due to its relatively high Mcl1 affinity. Studies to validate the efficacy of Mcl1 targeting in vivo are currently underway. Finally, although these data indicate that Mcl1 plays a prominent pro-survival function, NBs are expected to heterogeneously express BH survival proteins to subvert apoptosis. It remains possible, therefore, that alternative pro-survival proteins are operative in some tumor subsets. Thus, functional characterization of responses to BH antagonism in a broader array of NB may prove important in predicting which targeting strategies are most likely to be clinically efficacious.

Materials and Methods

Tumor tissue microarray (TMA)

A paraffin-embedded TMA was used to assess protein expression by immunohistochemistry (IHC). The TMA includes 185 human neuroblastic tumor cores (0.6 mm) arrayed in duplicate as previously described. Tumors were classified using the International Neuroblastoma Pathology Classification (INPC) system. For IHC, TMA sections were microwaved for 5 min in 0.01 M citrate buffer (pH 7.6) and blocked in 0.1 M Tris buffer with 2% fetal bovine serum (FBS). Slides were incubated with antibodies against human Mcl1 (S-19) or Bcl2 (100) (Santa Cruz Biotechnology, Santa Cruz, CA) at 1:1,000 dilution for 30 min, followed by biotinylated anti-rabbit IgG (1:200) and avidin-biotin complex (Vector Laboratories, Burlingame, CA). Slides were developed with DAB (Dako, Carpenteria, CA) and counterstained with hematoxylin.

TMA staining was graded semiquantitatively using a four-tiered scale (0: no staining, +1: <25% of cells stained, +2: 25–75% stained, +3: >75% stained). Expression was considered “high” if any tumor core scored +3, and “present” if at least one of two duplicate cores scored +3, or if both cores scored at least +2. Tumor cores inevaluable for a given BH protein were excluded from the analysis for that protein.

Cell culture and proliferation assays

High-risk NB-derived cell lines were grown in RMPI 1640 cell culture medium (Invitrogen, Carlsbad, CA) supplemented with 10% FBS, 5 mM glutamine, 1,000 U/mL penicillin, 1,000 μg/mL streptomycin and 250 μg⁄mL gentamicin. Adherent cells were detached with Versene (8 g/L NaCl, 0.2 g/L KCl, 1.15 g/L Na_2PO4, 0.2 g/L EDTA, 0.1 g/L Phenol red, pH 7.34), pelleted and resuspended in growth medium free of antibiotics. Cells were counted by hemocytometer and plated into 96-well plates on the Real-Time Cellular Electronic Sensing (RT-CES) system (Roche Diagnostics, Indianapolis, IN). This platform measures cell biomass proportional to viable cell number (cell index, CI) by determining changes in impedance, and is well-suited to the study of adherent NB cell lines.[38] The assay is reporter-free, allowing continuous growth monitoring under a variety of applied conditions. Plating densities varied from 10,000 to 30,000 cells/well as determined for each cell line.

Neural RPE1-hTERT cells were used as a control cell line, cultured as above except that DMEM/F12 (Invitrogen) +10% FBS was used as the growth medium. Also, RPE1 required trypsinization (1X trypsin-EDTA, Sigma-Aldrich, St. Louis, MO) for detachment. For RT-CES, RPE1 was plated at 6,000 cells/well.

RNA interference (RNAi)

Small inhibitory RNAs (siRNA) directed against Mcl1 (siMCL1), Bcl2 (siBCL2) and GapDH (siGDH) were purchased from Thermo Scientific Dharmacon (OnTargetPLUS SmartPool; Lafayette, CO) and used according to the manufacturer’s instructions. Briefly,

siRNA were reconstituted and stored at −80°C. Working dilutions were prepared in cell culture medium free of serum and antibiotics, and incubated for 20 minutes at room temperature with DharmaFect lipid transfection reagent. siRNAs were further diluted to final concentrations (5–100 nM) in media containing 10% FBS. Plating media was gently aspirated, and replaced with 100 μl of siRNA solution. All transfections were performed 24 or 48 hours after cell plating, when cells were in exponential growth and the CI measured ~1–2. Cell morphology was determined by phase microscopy in parallel experiments. Each experimental condition was independently replicated at least twice.

Q-RT-PCR and immunoblot analyses

To confirm the degree of knockdown by siRNA, we used Q-RT-PCR to semi-quantify mRNA levels in transfected versus untreated NB cell lines. Cell transfectants were collected 48 hours after application of siRNA, and RNA purified using the Quiagen RNeasy Mini kit according to manufacturer's instructions, including an on-column DNAse I digestion step. cDNA was synthesized from whole cell RNA using the SuperScript III First Strand kit (Invitrogen), and checked for integrity by agarose gel electrophoresis. Q-RT-PCR was performed on an Applied Biosystems 7900-HT instrument, using primer-probes for Mcl1, Bcl2, GapDH, SDHA and HPRT, and the TaqMan® Universal PCR Master Mix (Applied Biosystems, Foster City, CA). Relative mRNA was quantified using standard curves constructed from fetal brain RNA, and normalized to total cellular mRNA content using the geometric mean of SDHA and HPRT as neural housekeeping genes.[39]

Whole cell lysates for immunoblotting were collected from siRNA transfected or untreated cells grown to near-confluence in T-75 culture flasks, 48 hours after transfection. Cells were detached, rinsed in cold phosphate buffered saline (Invitrogen), and re-pelleted. Cell pellets were lysed in HEPES buffer (pH 7.7) containing 1% NP-40 and fresh Complete® protease inhibitor (Roche Applied Science, Mannheim, Germany), and homogenized by repeated passage through a 26G tuberculin needle. Lysates were incubated ≥24 hours at 4°C, then centrifuged at 14,000 g for 15 minutes. Protein content was determined by colorimetric assay (Bio-Rad, Hercules, CA) and equal amounts of protein were loaded onto 12% SDS-polyacrylamide gels (Invitrogen) and transferred to a PVDF blotting membrane (Invitrogen). Primary anti-human antibodies were: Mcl1 rabbit polyclonal (1:500; Santa Cruz), Bcl2 mouse monoclonal (1:1,000; Dako), caspase-9 rabbit polyclonal (1:1,000; Cell Signaling, Danvers, MA), β-tubulin mouse monoclonal (1:1,000; Sigma-Aldrich). Chemiluminescence was the detection method, using species-appropriate alkaline phosphatase (AP)-conjugated secondary antibodies and ImmunStar™ AP substrate (Bio-Rad). For densitometric estimation of caspase-9 cleavage, unmanipulated immunoblot images were digitized using U-SCAN-IT gel v. 6.1 (Silk Scientific Corp., Orem, UT) and expressed as (r), the ratio of pixel intensities of the 37 kDa band to the 47 kDa band.

In vitro cytotoxicity assays

The selective Bcl2-family antagonists ABT-737 and AT-101 were provided by Abbott Laboratories (Abbott Park, IL) and Ascenta Therapeutics (Malvern, PA), respectively. Stock solutions (20 mM) were prepared in DMSO and stored at −20°C. Final dilutions were prepared in complete or antibiotic-free medium immediately prior to use. At the time of drug addition, media was gently aspirated from wells and replaced with 100 μL of fresh media containing drug. Cell growth was monitored continuously over 72–96 hours using RT-CES.

For studies combining RNAi with conventional cytotoxics or small molecule antagonists, cells were pre-transfected for 24 hours with 5 nM (siMCL1) or 50 nM (siBCL2, siGDH) siRNA. After 24 hours, transfection media was replaced with an equal volume of media containing either etoposide (stock concentration 20 mg/ mL; Teva Pharmaceuticals, North

Wales, PA), doxorubicin (stock concentration 2 mg/mL; Bedford Laboratories, Bedford, OH), ABT-737 or AT-101. Cell growth was monitored by RT-CES. Each experimental condition was independently replicated in triplicate.

Statistical analysis

Tests of significance for Mcl1 and Bcl2 expression by TMA were conducted using Fishers exact test. For analysis by COG risk group, intermediate- and low-risk tumors were combined to increase statistical power. Survival analysis was conducted by the method of Kaplan and Meier, and significance determined by log-rank test. For in vitro cytotoxicity assays, pairwise comparisons of siMCL1 treatment versus siGDH control within each drug concentration were conducted using two-sided student's t-test. A cutoff of $a < 0.05$ was considered significant for all tests.

Supplementary Material

Refer to Web version on PubMed Central for supplementary material.

Acknowledgments

The authors thank Eric Rappaport and the Nucleic Acids and Protein Core facility for technical assistance with Q-RT-PCR, and Kristina Cole and John Maris for provision and annotation of the neuroblastoma TMA. Statistical analysis was supported by the CHOP-Westat Biostatistics and Data Management Core. ABT-737 was provided by Abbott Laboratories, and AT-101 by Ascenta Therapeutics.

Funding to support this work was provided by the National Institutes of Health CA97323, the Richard and Sheila Sanford Endowed Chair in Pediatric Oncology and the King Family (M.D.H.); The Caitlin Robb Foundation (M.N.F.); and the Daisy Day Fund (B.J.L.).

References

1. Goldsmith KC, Hogarty MD. Targeting programmed cell death pathways with experimental therapeutics: opportunities in high-risk neuroblastoma. Cancer Lett. 2005; 228:133–141. [PubMed: 15927359]
2. Obexer P, Geiger K, Ambros PF, Meister B, Ausserlechner MJ. FKHRL1-mediated expression of Noxa and Bim induces apoptosis via the mitochondria in neuroblastoma cells. Cell Death Differ. 2007; 14:534–547. [PubMed: 16888645]
3. Fulda S, Susin SA, Kroemer G, Debatin KM. Molecular ordering of apoptosis induced by anticancer drugs in neuroblastoma cells. Cancer Research. 1998; 58:4453–4460. [PubMed: 9766678]
4. Paffhausen T, Schwab M, Westermann F. Targeted MYCN expression affects cytotoxic potential of chemotherapeutic drugs in neuroblastoma cells. Cancer Lett. 2007; 250:17–24. [PubMed: 17141950]
5. Ushmorov A, Hogarty MD, Liu X, Knauss H, Debatin KM, Beltinger C. N-myc augments death and attenuates protective effects of Bcl-2 in trophically stressed neuroblastoma cells. Oncogene. 2008; 27:3424–3434. [PubMed: 18193081]
6. Hogarty MD. The requirement for evasion of programmed cell death in neuroblastomas with MYCN amplification. Cancer Letters. 2003; 197:173–179. [PubMed: 12880978]
7. Reed JC. Regulation of apoptosis by bcl-2 family proteins and its role in cancer and chemoresistance. Current Opinion in Oncology. 1995; 7:541–546. [PubMed: 8547403]
8. Letai AG. Diagnosing and exploiting cancer's addiction to blocks in apoptosis. Nat Rev Cancer. 2008; 8:121–132. [PubMed: 18202696]
9. Gojo I, Zhang B, Fenton RG. The cyclin-dependent kinase inhibitor flavopiridol induces apoptosis in multiple myeloma cells through transcriptional repression and downregulation of Mcl-1. Clin Cancer Res. 2002; 8:3527–3538. [PubMed: 12429644]
10. Paoluzzi L, Gonen M, Gardner JR, Mastrella J, Yang D, Holmlund J, et al. Targeting Bcl-2 family members with the BH3 mimetic AT-101 markedly enhances the therapeutic effects of

chemotherapeutic agents in in vitro and in vivo models of B-cell lymphoma. Blood. 2008; 111:5350–5358. [PubMed: 18292288]

11. Wolter KG, Verhaegen M, Fernandez Y, Nikolovska-Coleska Z, Riblett M, de la Vega CM, et al. Therapeutic window for melanoma treatment provided by selective effects of the proteasome on Bcl-2 proteins. Cell Death Differ. 2007; 14:1605–1616. [PubMed: 17541428]
12. Thallinger C, Wolschek MF, Maierhofer H, Skvara H, Pehamberger H, Monia BP, et al. Mcl-1 is a novel therapeutic target for human sarcoma: synergistic inhibition of human sarcoma xenotransplants by a combination of mcl-1 antisense oligonucleotides with low-dose cyclophosphamide. Clin Cancer Res. 2004; 10:4185–4191. [PubMed: 15217956]
13. Song L, Coppola D, Livingston S, Cress D, Haura EB. Mcl-1 regulates survival and sensitivity to diverse apoptotic stimuli in human non-small cell lung cancer cells. Cancer Biol Ther. 2005; 4:267–276. [PubMed: 15753661]
14. Janoueix-Lerosey I, Schleiermacher G, Michels E, Mosseri V, Ribeiro A, Lequin D, et al. Overall genomic pattern is a predictor of outcome in neuroblastoma. J Clin Oncol. 2009; 27:1026–1033. [PubMed: 19171713]
15. Mosse YP, Greshock J, Margolin A, Naylor T, Cole K, Khazi D, et al. High-resolution detection and mapping of genomic DNA alterations in neuroblastoma. Genes Chromosomes Cancer. 2005; 43:390–403. [PubMed: 15892104]
16. Hackett CS, Hodgson JG, Law ME, Fridlyand J, Osoegawa K, de Jong PJ, et al. Genome-wide array CGH analysis of murine neuroblastoma reveals distinct genomic aberrations which parallel those in human tumors. Cancer Research. 2003; 63:5266–5273. [PubMed: 14500357]
17. Ammann JU, Haag C, Kasperczyk H, Debatin KM, Fulda S. Sensitization of neuroblastoma cells for TRAIL-induced apoptosis by NFkappaB inhibition. Int J Cancer. 2009; 124:1301–1311. [PubMed: 19065652]
18. Nakamura Y, Ozaki T, Niizuma H, Ohira M, Kamijo T, Nakagawara A. Functional characterization of a new p53 mutant generated by homozygous deletion in a neuroblastoma cell line. Biochem Biophys Res Commun. 2007; 354:892–898. [PubMed: 17276397]
19. Zhai D, Jin C, Satterthwait AC, Reed JC. Comparison of chemical inhibitors of anti-apoptotic Bcl-2-family proteins. Cell Death Differ. 2006; 13:1419–1421. [PubMed: 16645636]
20. Tse C, Shoemaker AR, Adickes J, Anderson MG, Chen J, Jin S, et al. ABT-263: a potent and orally bioavailable Bcl-2 family inhibitor. Cancer Res. 2008; 68:3421–3428. [PubMed: 18451170]
21. Lock R, Carol H, Houghton PJ, Morton CL, Kolb EA, Gorlick R, et al. Initial testing (stage 1) of the BH3 mimetic ABT-263 by the pediatric preclinical testing program. Pediatr Blood Cancer. 2008; 50:1181–1189. [PubMed: 18085673]
22. Konopleva M, Contractor R, Tsao T, Samudio I, Ruvolo PP, Kitada S, et al. Mechanisms of apoptosis sensitivity and resistance to the BH3 mimetic ABT-737 in acute myeloid leukemia. Cancer Cell. 2006; 10:375–388. [PubMed: 17097560]
23. Kang MH, Wan Z, Kang YH, Sposto R, Reynolds CP. Mechanism of synergy of N-(4-hydroxyphenyl)retinamide and ABT-737 in acute lymphoblastic leukemia cell lines: Mcl-1 inactivation. J Natl Cancer Inst. 2008; 100:580–595. [PubMed: 18398104]
24. van Delft MF, Wei AH, Mason KD, Vandenberg CJ, Chen L, Czabotar PE, et al. The BH3 mimetic ABT-737 targets selective Bcl-2 proteins and efficiently induces apoptosis via Bak/Bax if Mcl-1 is neutralized. Cancer Cell. 2006; 10:389–399. [PubMed: 17097561]
25. Lin X, Morgan-Lappe S, Huang X, Li L, Zakula DM, Vernetti LA, et al. 'Seed' analysis of off-target siRNAs reveals an essential role of Mcl-1 in resistance to the small-molecule Bcl-2/Bcl-X_L inhibitor ABT-737. Oncogene. 2007; 26:3972–3979. [PubMed: 17173063]
26. Wang G, Nikolovska-Coleska Z, Yang CY, Wang R, Tang G, Guo J, et al. Structure-based design of potent small-molecule inhibitors of anti-apoptotic Bcl-2 proteins. J Med Chem. 2006; 49:6139–6142. [PubMed: 17034116]
27. Chesler L, Goldenberg DD, Collins R, Grimmer M, Kim GE, Tihan T, et al. Chemotherapy-induced apoptosis in a transgenic model of neuroblastoma proceeds through p53 induction. Neoplasia. 2008; 10:1268–1274. [PubMed: 18953436]
28. Zhu X, Wimmer K, Kuick R, Lamb BJ, Motyka S, Jasty R, et al. N-myc modulates expression of p73 in neuroblastoma. Neoplasia (New York NY, United States). 2002; 4:432–439.

29. Haber M, Smith J, Bordow SB, Flemming C, Cohn SL, London WB, et al. Association of high-level MRP1 expression with poor clinical outcome in a large prospective study of primary neuroblastoma. J Clin Oncol. 2006; 24:1546–1553. [PubMed: 16575006]

30. Goldsmith KC, Liu X, Dam V, Morgan BT, Shabbout M, Cnaan A, et al. BH3 peptido-mimetics potently activate apoptosis and demonstrate single agent efficacy in neuroblastoma. Oncogene. 2006; 25:4525–4533. [PubMed: 16568093]

31. Mason KD, Vandenberg CJ, Scott CL, Wei AH, Cory S, Huang DC, et al. In vivo efficacy of the Bcl-2 antagonist ABT-737 against aggressive Myc-driven lymphomas. Proc Natl Acad Sci USA. 2008; 105:17961–17966. [PubMed: 19004807]

32. Kurata K, Yanagisawa R, Ohira M, Kitagawa M, Nakagawara A, Kamijo T. Stress via p53 pathway causes apoptosis by mitochondrial Noxa upregulation in doxorubicin-treated neuroblastoma cells. Oncogene. 2008; 27:741–754. [PubMed: 17653088]

33. Carr J, Bell E, Pearson AD, Kees UR, Beris H, Lunec J, et al. Increased frequency of aberrations in the p53/MDM2/p14(ARF) pathway in neuroblastoma cell lines established at relapse. Cancer Res. 2006; 66:2138–2145. [PubMed: 16489014]

34. Okumura K, Huang S, Sinicrope FA. Induction of Noxa sensitizes human colorectal cancer cells expressing Mcl-1 to the small-molecule Bcl-2/Bcl-x_L inhibitor, ABT-737. Clin Cancer Res. 2008; 14:8132–8142. [PubMed: 19088028]

35. Tahir SK, Yang X, Anderson MG, Morgan-Lappe SE, Sarthy AV, Chen J, et al. Influence of Bcl-2 family members on the cellular response of small-cell lung cancer cell lines to ABT-737. Cancer Res. 2007; 67:1176–1183. [PubMed: 17283153]

36. Wei SH, Dong K, Lin F, Wang X, Li B, Shen JJ, et al. Inducing apoptosis and enhancing chemosensitivity to gemcitabine via RNA interference targeting Mcl-1 gene in pancreatic carcinoma cell. Cancer Chemother Pharmacol. 2008; 62:1055–1064. [PubMed: 18297287]

37. Winter C, Pawel B, Seiser E, Zhao H, Raabe E, Wang Q, et al. Neural cell adhesion molecule (NCAM) isoform expression is associated with neuroblastoma differentiation status. Pediatr Blood Cancer. 2008; 51:10–16. [PubMed: 18213713]

38. Mosse YP, Laudenslager M, Longo L, Cole KA, Wood A, Attiyeh EF, et al. Identification of ALK as a major familial neuroblastoma predisposition gene. Nature. 2008; 455:930–935. [PubMed: 18724359]

39. Fischer M, Skowron M, Berthold F. Reliable transcript quantification by real-time reverse transcriptase-polymerase chain reaction in primary neuroblastoma using normalization to averaged expression levels of the control genes HPRT1 and SDHA. J Mol Diagn. 2005; 7:89–96. [PubMed: 15681479]

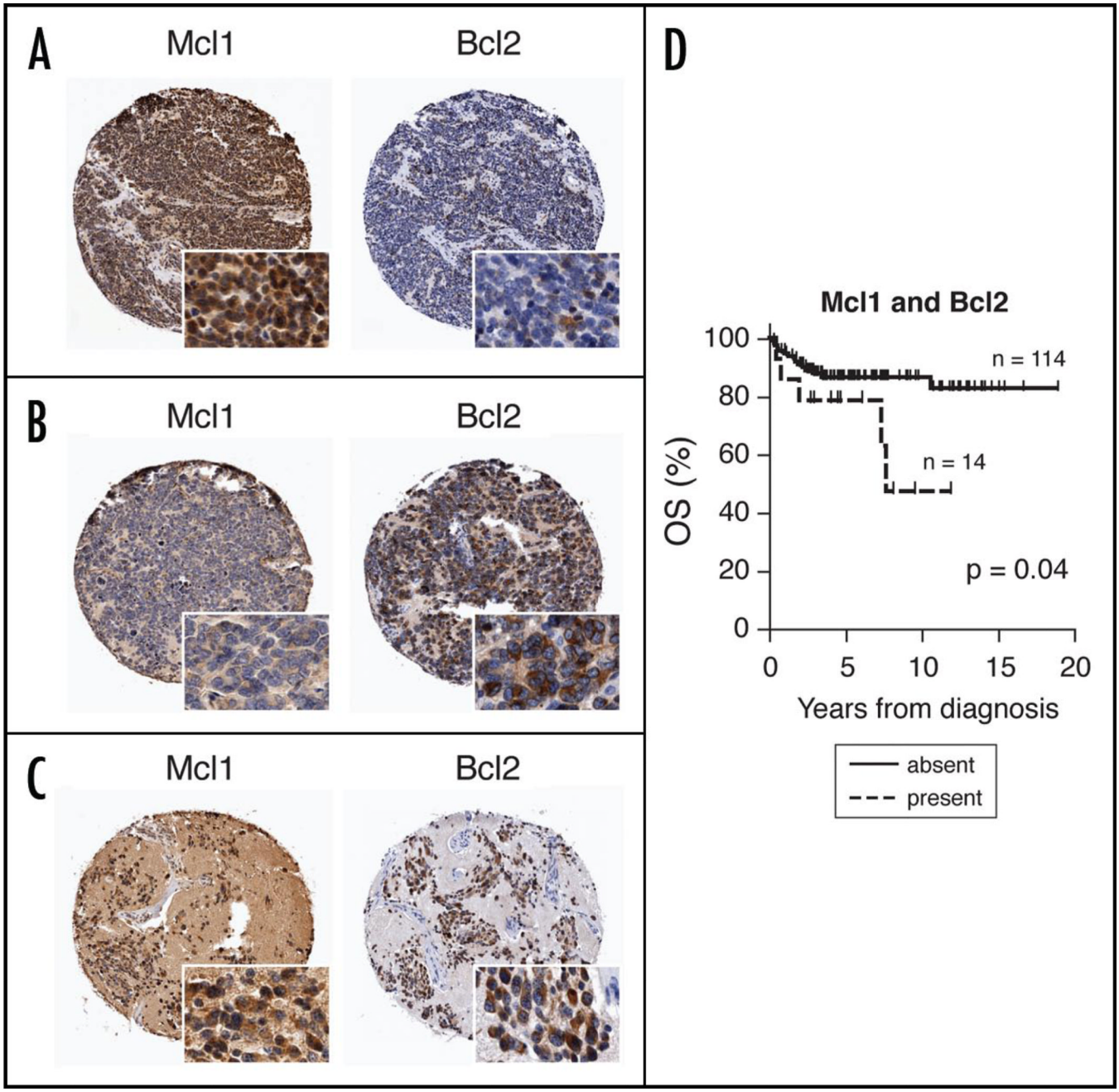

Figure 1.

Three representative cores from Human NB tumor tissue microarray (TMA) demonstrating (A) high Mcl1, low Bcl2; (B) low Mcl1, high Bcl2; and (C) dual high Mcl1, Bcl2 expression. Insets show subcellular localization of IHC staining (original magnification = 20x). (D) Kaplan-Meier curve depicting worse OS in patients whose tumors express both Mcl1 and Bcl2 by IHC.

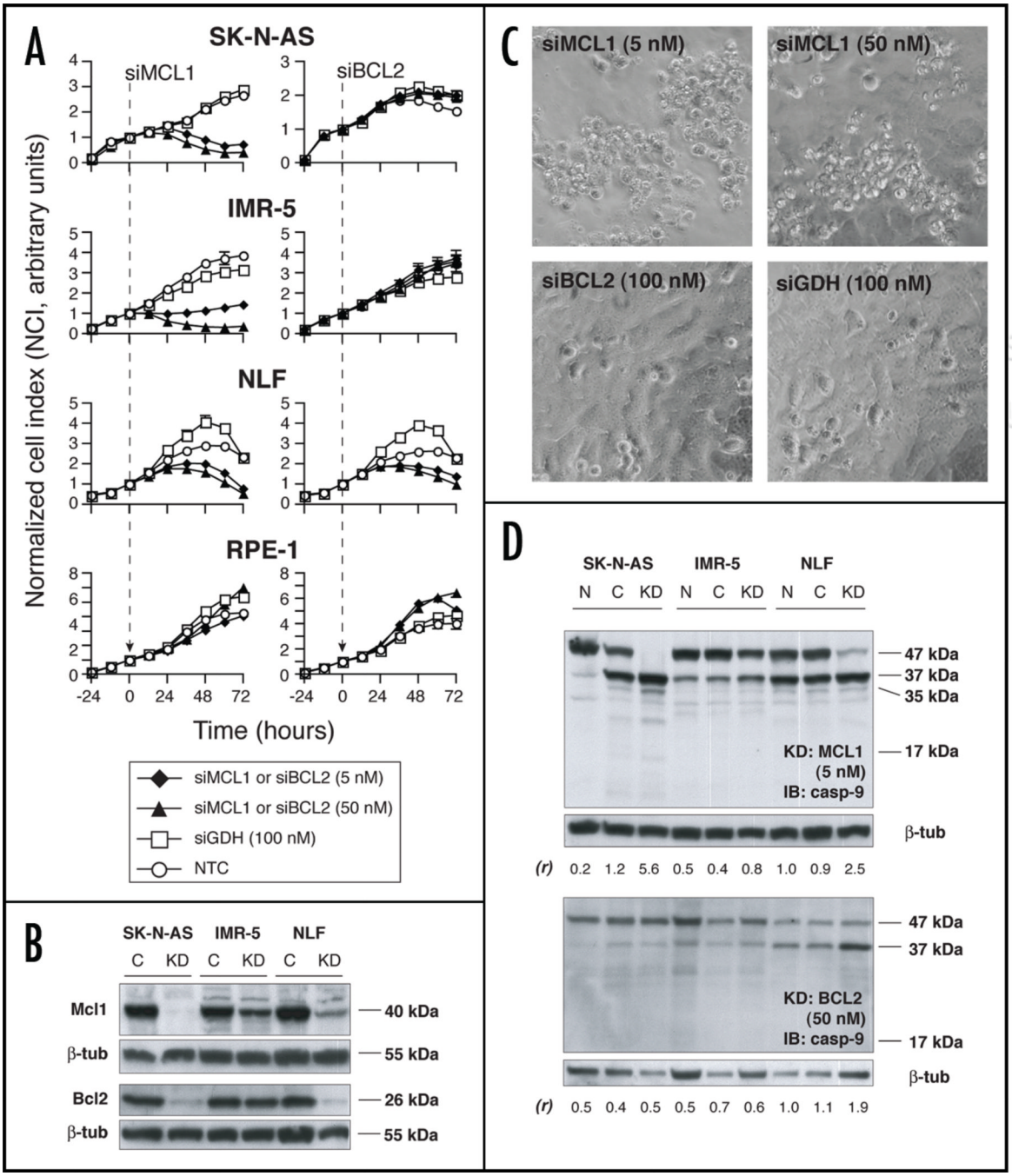

Figure 2.

(A) siRNA knockdown of Mcl1 (left) and Bcl2 (right) in NB cell lines and in the control cell line RPE-1 (♦ = 5 nM siMCL1 or siBCL2; ▲ = 50 nM siMCL1 or siBCL2; □ = 100 nM siGDH; ○ = nontreated control, NTC). Graphs are representative of at least 2 independent experiments, and depict mean of duplicate wells ±SEM (error bars may be smaller than symbol). (B) Protein immunoblot showing effectiveness of translational inhibition in siMCL1 or siBCL2-treated cells (knockdown, "KD") versus siGDH-treated control ("C"). siRNA concentrations were 5 nM for siMCL1 and 50 nM for siBCL2. (C) Phase contrast microscopy in siRNA-treated SK-N-AS demonstrates that siMCL1 treatment resulted in a refractile, fragmented cellular morphology (upper). In contrast, cell monolayers grew to

confluence and exhibited normal morphology with both siBCL2 and siGDH treatment (lower). (D) Protein immunoblots showing caspase-9 cleavage in response to siRNA treatment. Upper: cells treated with siMCL1 ("KD," 5 nM) demonstrate loss of full-length procaspase-9 (47 kDa) and increase in 37 kDa, 35 kDa and 17 kDa cleavage products versus NTC ("N") and siGDH treatment ("C," 100 nM). Lower: only NLF demonstrates increased caspase-9 cleavage with siBCL2 treatment ("KD", 50 nM), consistent with cell growth assays. Ratios of the relative intensities of the 37 kDa/47 kDa bands are shown as (*r*), with higher (*r*) indicating a greater degree of caspase-9 processing.

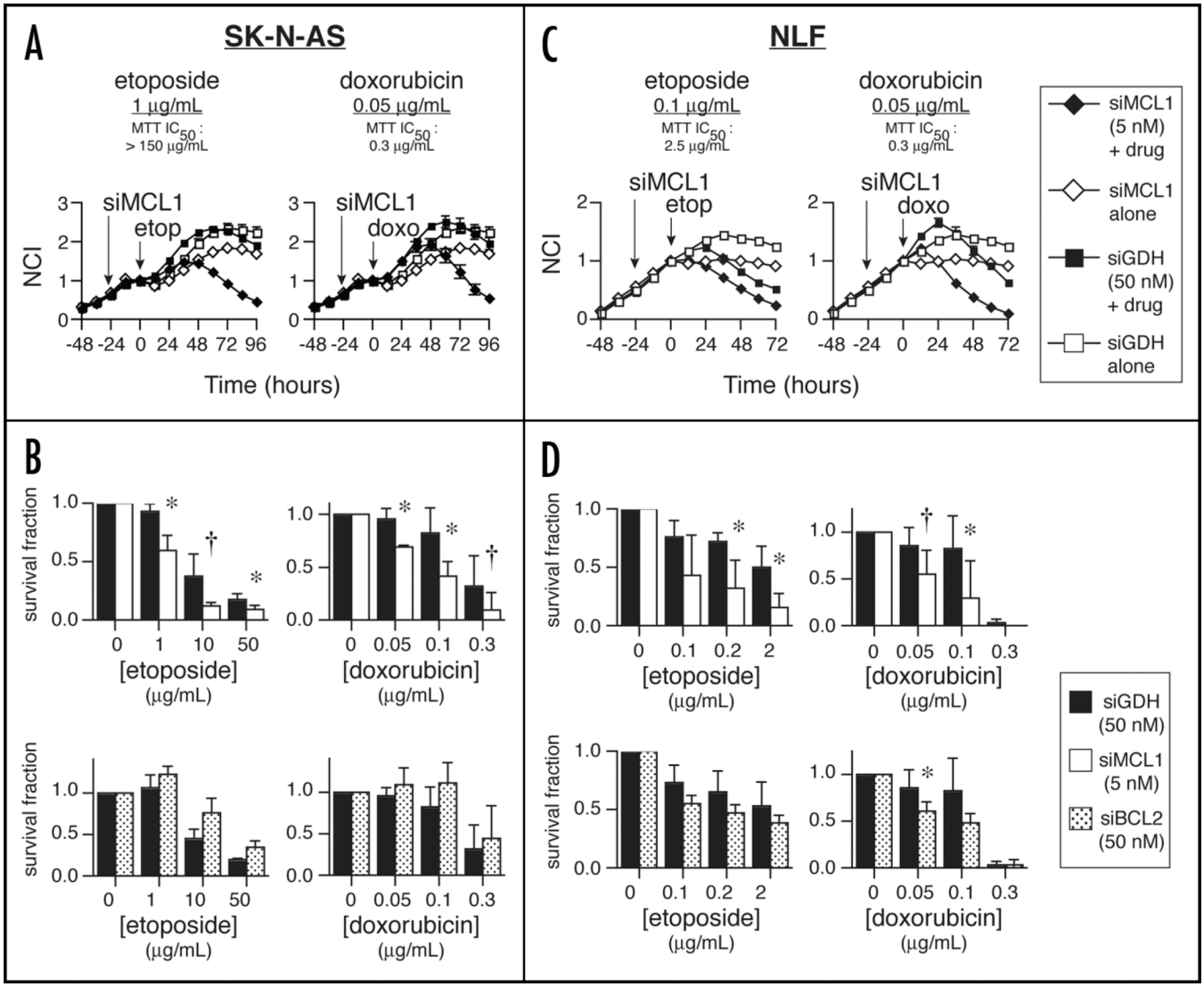

Figure 3.

In vitro combination of siRNA and cytotoxics in NB cell lines. (A) RT-CES survival data in SK-N-AS shows potentiation of etoposide (left, ' = 1 µg/mL) or doxorubicin (right, ' = 0.05 µg/mL) by 24-hour siMCL1 pre-treatment (♦ = 5 nM), versus combination therapy with siGDH (□ = 50 nM) or with siMCL1 alone (◊ = 5 nM). For clarity, one representative RT-CES curve from multiple independent experiments is depicted. (B) Aggregate survival data for SK-N-AS after 48 hours of treatment with chemotherapy and 24-hour pre-treatment with siGDH (' = 50 nM), siMCL1 (□ = 5 nM) or siBCL2 (11 = 50 nM). (C) Results of chemotherapy treatment in NLF combined with MCL1 knockdown. Symbols are the same as in (A), except (' = 0.1 µg/ mL etoposide). (D) Aggregate 48-hour survival data in NLF, as described in (B). Bcl2 knockdown trended toward additivity in NLF, but did not reach statistical significance except for doxorubicin at 0.05 µg/mL. For (B and D), bars represent mean ± SD of 3 independent experiments; * = pairwise 2-sided $p \leq 0.05$; † = $0.05 < p \leq 0.1$.

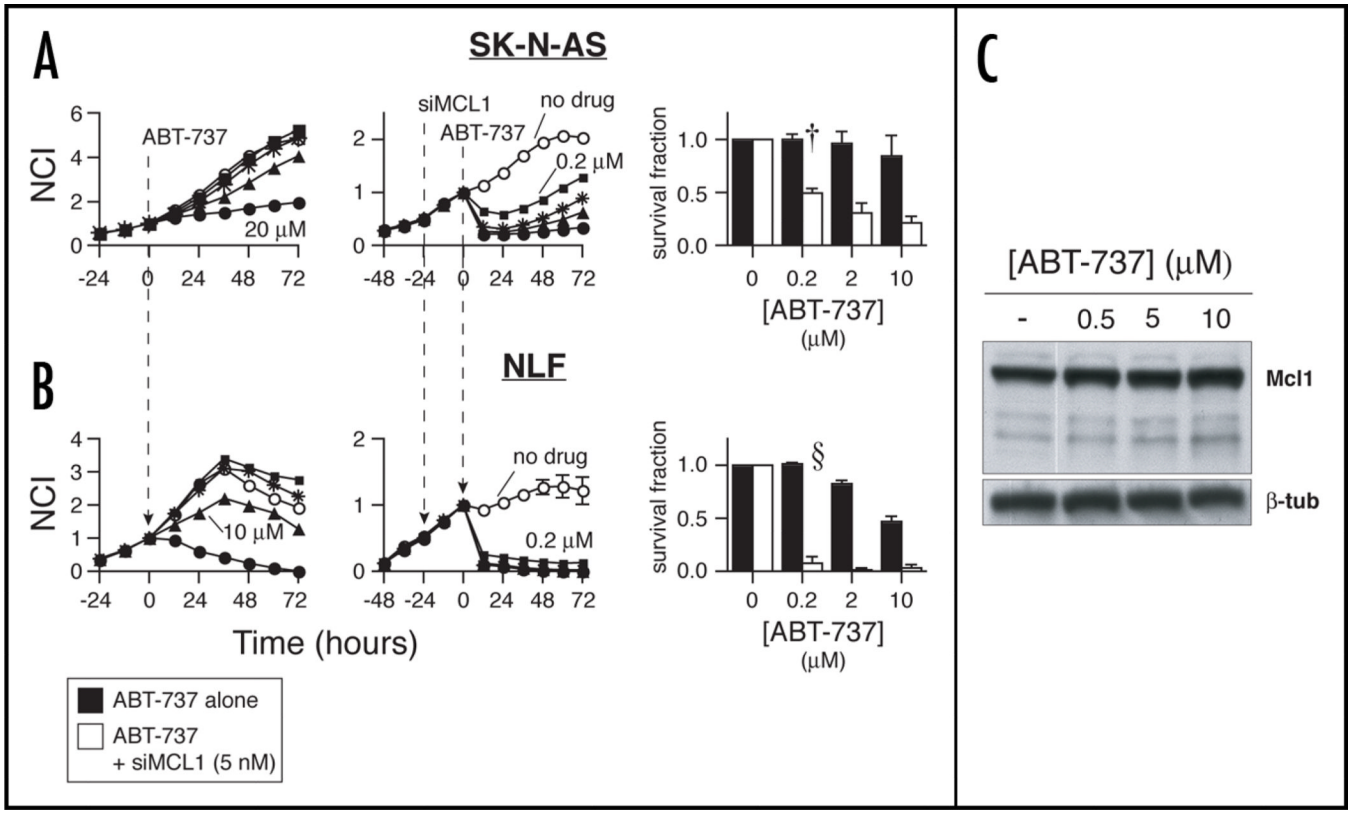

Figure 4.

Mcl1 KD sensitizes resistant NB to ABT-737. (A) RT-CES dose-response relationships in SK-N-AS with ABT-737 alone (left graph) or in combination with 24-hour siMCL1 pretreatment (middle graph). ABT-737 concentration symbol legend: ○ = 0 μM (media or siMCL1 alone); ▪ = 0.2 μM; * = 2 μM; ▲ = 10 μM; ● = 20 μM. Aggregate 48-hour survival data (right graph), with ABT-737 alone (▪) or in combination with 24-hour Mcl1 knockdown (□). (B) ABT-737 alone shows similar activity in NLF, with marked sensitization seen when Mcl1 is silenced. Concentration symbols are as for SK-N-AS. Aggregate 48-hour survival data for NLF demonstrates near-complete cell death at ABT-737 concentration = 200 nM in combination with Mcl1 knockdown. n = 3 independent experiments; † = pairwise $p \leq 6E\text{-}3$; $^{\S}p \leq 2.3E\text{-}4$. (C) Immunoblot showing high basal Mcl1 expression in SK-N-AS, and lack of substantial induction by ABT-737 at 6 hours.

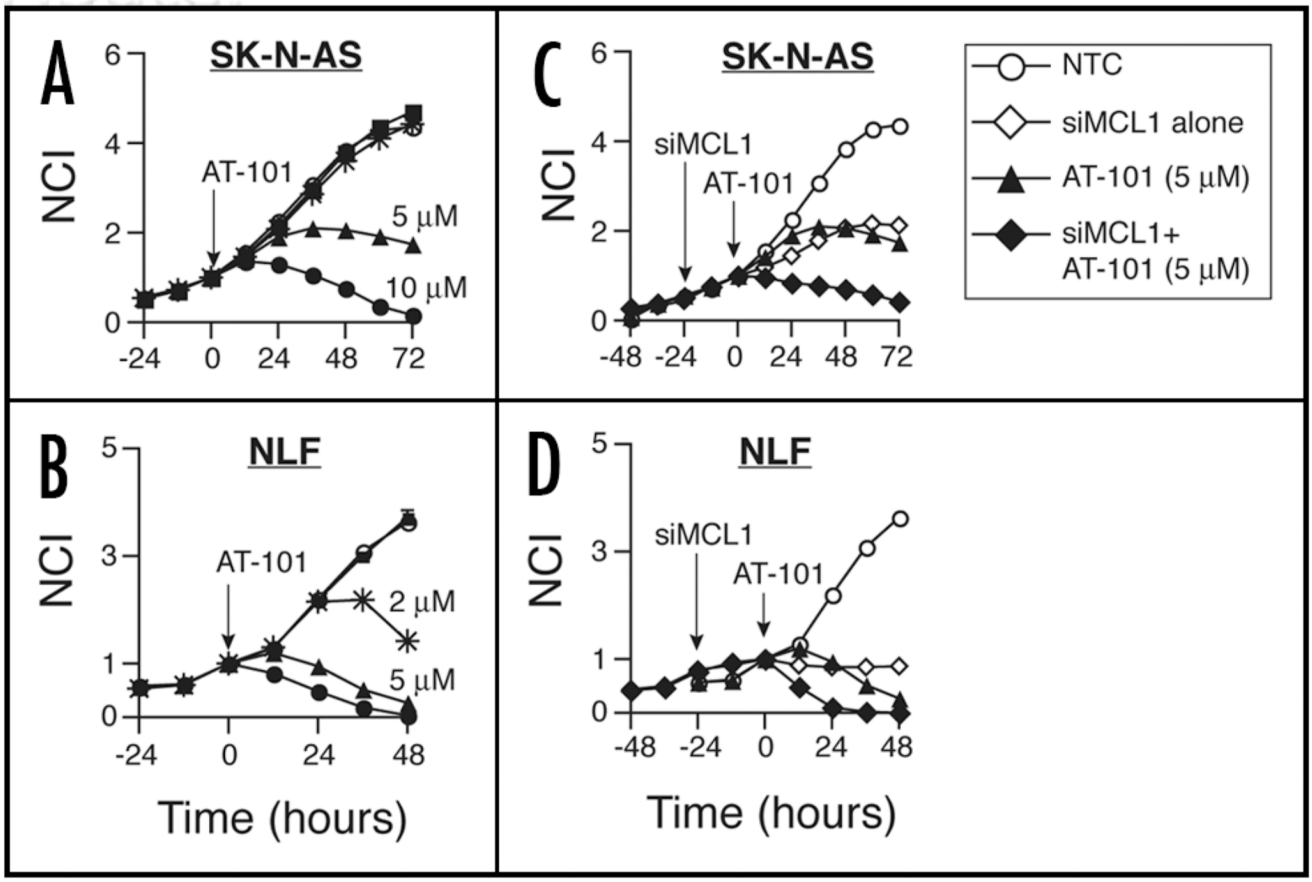

Figure 5.

Activity of AT-101 in (A) SK-N-AS and (B) NLF. AT-101 concentration symbol legend: ○ = 0 μM (media alone); ' = 0.2 μM; * = 2 μM; ▲ = 5 μM; ●= 10 μM. (C and D): 24 hours of Mcl1 knockdown augments the early response to AT-101 at intermediate concentrations. ▲ = 5 μM AT-101; ◆ = 5 μM AT-101 with 5 nM siMCL1; ◊ = *5* nM siMCL1 alone; ○ = media. Curves are representative of at least 2 independent experiments.

Table 1

Pro-survival BH protein expression frequencies in human NB tumor tissue microarray

			Mcl1				Bcl2				Mcl1 or Bcl2				Mcl1 and Bcl2			
		n (%)	**present (%)**	**p***	**high (%)**	**p**	**present (%)**	**p**	**high (%)**	**p**	**present (%)**	**p**	**high (%)**	**p**	**present (%)**	**p**	**high (%)**	**p**
All		165	42/134		18/134		48/154		24/154		78/138		36/132		14/128		6/128	
			(31)		(13)		(31)		(16)		(57)		(27)		(11)		(5)	
Risk Group	**H**	35	10/24	1.0	5/24	0.54	16/32	**0.02**	9/32	0.16	21/26	**0.05**	12/26	**0.08**	5/24	0.29	2/24	0.63
(N = 101)		(35)	(42)		(21)		(50)		(28)		(81)		(46)		(21)		(8)	
	IL	66	24/58		9/58		16/63		9/63		34/59		15/58		6/57		3/57	
		(66)	(41)		(16)		(25)		(14)		(58)		(26)		(11)		(5)	
MYCN Amp	**Y**	17	5/10	0.15	4/10	**0.03**	6/14	0.56	3/14	0.72	8/11	0.21	6/11	**0.07**	3/10	0.15	1/10	0.48
(N = 103)		(17)	(50)		(40)		(43)		(21)		(73)		(55)		(30)		(10)	
	N	86	20/75		8/75		29/84		15/84		40/78		19/77		9/74		4/74	
		(83)	(27)		(11)		(35)		(18)		(51)		(25)		(12)		(5)	

*Fisher's exact test.